

Influence of heat transport, deposits and condensor leakages upon corrosion in steam generators

W. M. M. Huijbregts* , J.H.N. Jelgersma* and A. Snel*

VGB Kraftwerkstechnik 55, 1, Jan. 1975, pp. 26/39.

* N.V. KEMA (joint laboratories electric utilities in The Netherlands) Utrechtseweg 310, Arnhem

1. Introduction

Waterside steam generator corrosion is generally the result of a number of unfavourable factors, such as too high heat flux, too low mass transport or too high fraction of steam in the tubes. presence of deposits on the surfaces and inadequate water quality. The influence of certain impurities in the boiler water upon corrosion can be thoroughly studied with experiments in autoclaves.

In order to be able to include the different dynamic factors in the general investigation of steam generation corrosion -heat flux, two-phase flow of the water-steam mixture and formation of deposits - N.V. KEMA has an experimental boiler installation.(Fig. 1).



Figure 1. Experimental 1 Mw boiler for corrosion experiments at KEMA (the Netherlands).

All imaginable waterside and steam side operating conditions of the various boiler types, such as natural circulation -and forced circulation boilers, once-through boilers and supercritical boilers, can be imitated and, if necessary, aggravated in the test sections of this boiler installation.

The corrosion investigations are subdivided into four phases with the following subjects:

1. Influence of heat transport upon the formation of protective oxide layers under various thermo-hydraulic conditions
2. Initiation of "on-load corrosion" by dosing oxide suspensions and sea-water salts under nucleate boiling and bubble-, plug- and annular flow.
3. Reducing "on-load corrosion" during sea water leakage by alkalisation with solids.
4. Corrosion susceptibility of various steel qualities and welds.

The first two phases of the study have been finished and some of the results will be discussed in more detail.

2. Design of the boiler Installation

The experimental boiler installation consists of a circuit in which water and steam, respectively, is circulating by means of a high-pressure pump.(Fig.2).

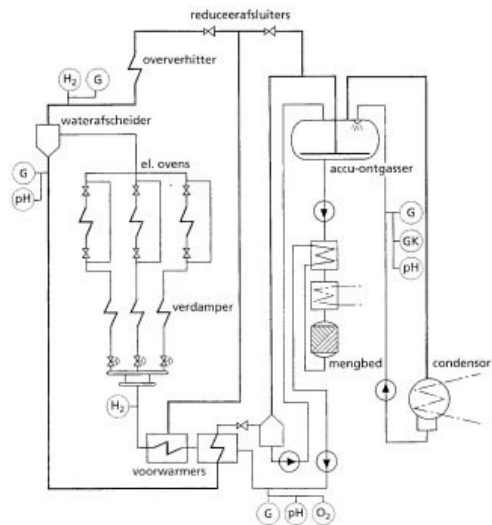


Figure 2. Water steam circuit of the experimental boiler.

Behind the feedwater pump and preheaters, the feedwater is divided into three lines which represent the pre-evaporator and in which a certain steam-water ratio can be maintained at a desired mass-flow and pressure (maximum values 2500 kg/h and 285 bar, respectively). With the three lines three test tubes are connected which are surrounded by radiation furnaces with a maximum output of about 400 kW/m².

Behind the test tubes, the emerging water-steam mixture is combined and led to a water separator. The water is by a cooler and after depressuring returned to the feed-water container, the steam is after superheating depressurized and condensed.

The test tubes are set up in vertical hinged swing-out radiation furnaces of 41 cm length (Fig. 3)



Figure 3. Test tube for heat-input measurements with opened furnace in test section II.

Each of the test sections I and III is equipped with one furnace, but section II has two furnaces of 41 cm length separated by an interval of 13 cm. The heating parts of sections I and III are thus about 40 cm long and those in section II about 80 cm long. The lower furnace in test section II was always adjusted to a 25% lower output than the upper furnace- The locations of the furnaces is indicated in the split halves of the tubes by black line markings (for example, Fig. 18).

For identification of the tubes the following method was used: The first number indicates the test number, the second number the tube number, the third number the distance to the lower flange of the test tube and the fourth number the distribution of hours of the furnace position around the tube circumference. The numbers are separated from each other by sloping lines.

In the test tubes for the corrosion investigation two thermo-couples (1 mm O.D.) are mounted at a height corresponding to the middle of the furnaces and at a distance of 2 mm and 5 mm from the internal tube surface. With the aid of these thermo-couples the local heat-flux density and the internal tube wall temperature are calculated.

2.1 Chemical supervision

For supervising the water quality the installation is equipped with many sample-taking locations and a measuring apparatus. For the corrosion experiments it is important to know the water composition at the inlet and outlet of the test tubes. For this purpose samples of the feedwater are taken at the inlet of the evaporator and of the boiler water at the outlet of the water separator. At these locations recording measurements are made during operation for determination of pH, O_2 , H_2 and conductivity. SiO_2 , Cu, Fe and Na are analysed one to three times per week. The hydrogen content is particularly measured in order to be able to determine exactly when severe corrosion in the test tube begins .

2.2 Heat transfer and flow of a water-steam mixture

In evaporator corrosion the heat-transfer phenomena at the tube wall are playing a very important role. For describing the testing conditions it is therefore necessary to know not only the water composition, but also the thermo-hydraulic conditions in the test section. Collier (1, 2) presents for the heat- transfer phenomena in a tube with a water-steam mixture flow the following model:

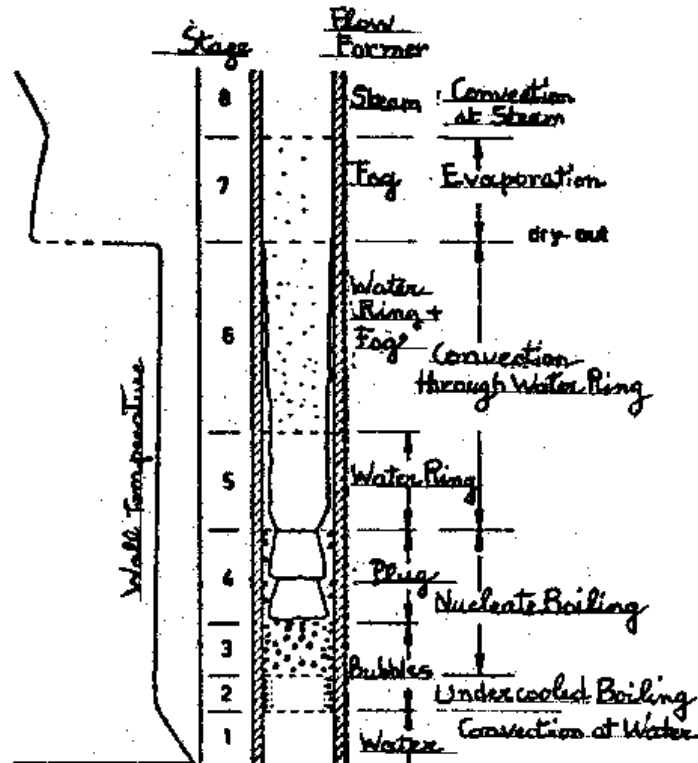


Figure 4.
Schematic representation of heat transfer and two-phase flow in boiler tube (Collier, 1966).

If water is conducted through a tube and one investigates the heating-up process until superheated steam has formed, various states are recognised at sufficiently high mass flow and not too high heat input (Fig. 4). The water is at the beginning undercooled and heat-transfer occurs then by convection. With increasing enthalpy undercooled boiling occurs. The bubbles condense in the center of the tube. In the third state the bubbles persist and combine to form steam plugs in the center, thereby crowding the water toward the tube surface. Although heat transfer still takes place in this water film by steam bubble formation (nucleate boiling), this process becomes with increasing steam-fraction controlled more and more by convection in the water film. The difference in the velocity of the water film on the tube surface and of the steam in the center becomes with increasing fraction of steam greater and greater. This causes that small water drops from the water film are carried along by the steam. The water film becomes thinner and thinner and finally dries out completely. This point is accordingly designated as "dry-out" point. It is associated with a temperature increase of the tube wall. The magnitude of this increase depends greatly on the mass-flow, the steam fraction and the heat-input. When all water drops in the steam are evaporated, the steam enters the superheated state.

If the heat-input is so high and the mass flow so low that the formed steam bubbles do not separate fast enough from the tube wall, a strongly heat-insulating steam film forms for a short time between the water and the tube wall accompanied by a high increase in the tube wall temperature. As soon as the steam film separates, the tube is again well cooled by the water, and the temperature drops. This process is called partial film boiling. Partial film boiling can cause very high temperature fluctuations. If the heat-input is so high that complete film boiling occurs (the steam film is then stable) the temperature will rise so much that the material ruptures. This phenomenon is called "burn-out". For "burn-out" as well as for "dry-out" there is at a certain flow condition a critical value for the heat-input.

Collier described the heat transfer phenomena in water-steam mixtures in which with increasing steam fraction bubble-flow (small steam bubbles in water) changed through plug-flow to annular flow

(presence of water film) and finally to fog-flow. It was found, however, that the flow picture of a water-steam mixture depends not only on the steam fraction, but also on the mass-transport and on the prevailing pressure. Rosler (3) has carried out measurements in rectangular tubes in order to establish the flow zone as function of pressure, mass-flow and steam fraction. Fig. 5 shows the various zones.

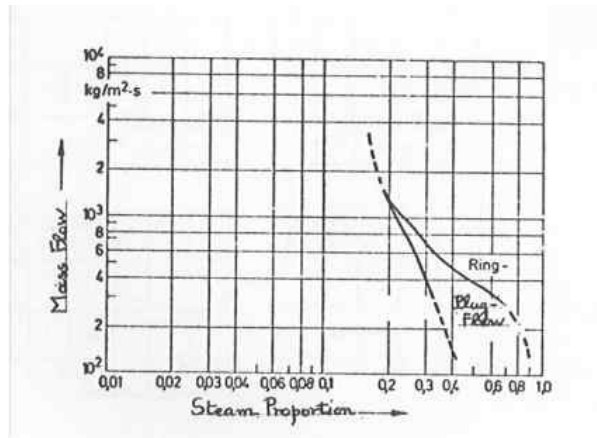
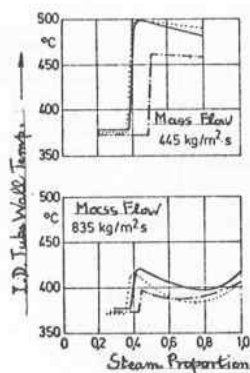


Figure 5. Flow in rectangular tubes at 140 bar (Rosler, 1966).

In order to know the thermohydraulic conditions in the test sections, we have carried out extensive heat-flux measurements before the start of the corrosion experiments, using a special calibration tube in which pairs of thermo-couples were mounted at various heights. It was found that the "dry-out" point is at a steam fraction of 0.37, notwithstanding the mass-transport. The tube wall temperature increase, however, decreases appreciably with increasing mass-transport. The heat-input was on all sides (Fig. 6).



.Figure 6. Heat-input measurements in a pickled tube with heating from all sides. Heat input 300 kW/m^2 . Location of thermocouples: distance from underside furnace (cm): _____ 4, ____ . ____ 14, ===== 24, 34.

At one side heat-flux the temperature-peak up to "dry-out" was less distinct, and the temperature increase of the tube wall likewise less high (Fig. 7).

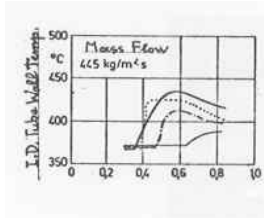


Figure 7. Heat-input measurements in a pickled tube with heating on one side only, Heat input 300 kW/m^2 . Location of thermocouples: distance from underside furnace (cm): _____ 4, _____ 14, _____ 24, 34

It is evident now that the critical steam fraction -the fraction of steam at which "dry-out" occurs - depends indeed on the mass-flow, but with increasing mass-transport the critical steam fraction shifts to somewhat higher values.

3. Phase 1 of evaporator corrosion investigation

In this phase, the influence of the thermohydraulic conditions upon the formation of a protective oxide layer has been studied with normal water condition. The thermohydraulic conditions have been chosen over a very great range: mass-transport of 1100 to $1900 \text{ kg/m}^2 \cdot \text{s}$, the steam fraction from 0.16 to 0.80 , and the heat-flux density from 30 to 400 kW/m^2 . Only pickled, clean and deposit-free tubes were used. All experiments were made at 180 bar . During the tests the tubes were heated over the entire circumference with only one furnace.

At the beginning, the boiler water did not completely meet the purity requirements for Dutch power plants. The SiO_2 -content and the conductivity were always too high. The requirements could only be met after starting the operation of the condensate purification installation, i. e. , after experiment No.25. With one exception (experiment No.32) the tests of this phase, too, were conducted with a higher SiO_2 -content in the boiler water (mean value about 60 ug/kg).The feedwater was maintained at a pH of about 9.2 with the use of NH_3 .

A great number of experiments were carried out. They can be divided into three large groups, depending on the flow conditions: bubble-flow, plug-flow and water-ring-flow. This division has been made according to the flow zones indicated by Rosler (Fig. 5) .Under normal conditions, only bubble-flow occurs in a modern circulation boiler. In a once-through boiler all three flow types are found.

3.1 Bubble-flow

Heat-input in these experiments was always below the critical value, at which "burn-out" can occur. Under the described water conditions (the only relatively high impurity was SiO_2), at none of the employed heat-inputs was appreciable corrosion found in the test tubes.

3.2 Plug-flow and annular flow

In the tubes which were exposed to plug-flow or annular flow, three types of deposits were formed, but without the occurrence of severe corrosion. These types are: pimples and pitting, local feather-shaped deposits and a homogeneous cover on the entire heat-input zone. The feather-shape deposits are found at "dry-out", pit formation at lower heat-inputs and the homogeneous deposit at higher mass-flows. Fig. 8 depicts an example of the three deposit types.

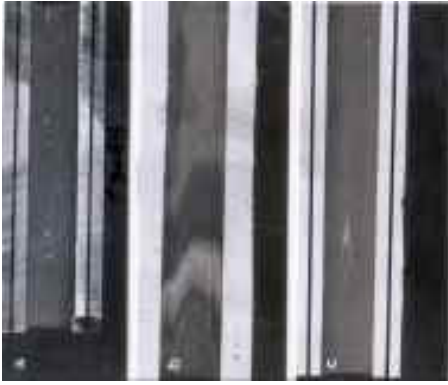


Figure 8. The 3 types of deposits: a) pimples, b) feather-shape deposits and c) homogeneous deposits.

The test results under plug-flow and annular flow conditions at an inlet steam fraction of 0.58 to 0.75 and 0.34 to 0.38 (see Table 1), are presented in two mass-flow/heat-input diagrams (Figs. 9 and 10) in which the deposit types found in the tubes are also indicated.

It is shown that there are four zones to be distinguished:
no deposits

1. pimple-form deposits
2. feather-shaped deposits ("dry-out" phenomena)
3. homogeneous covering.

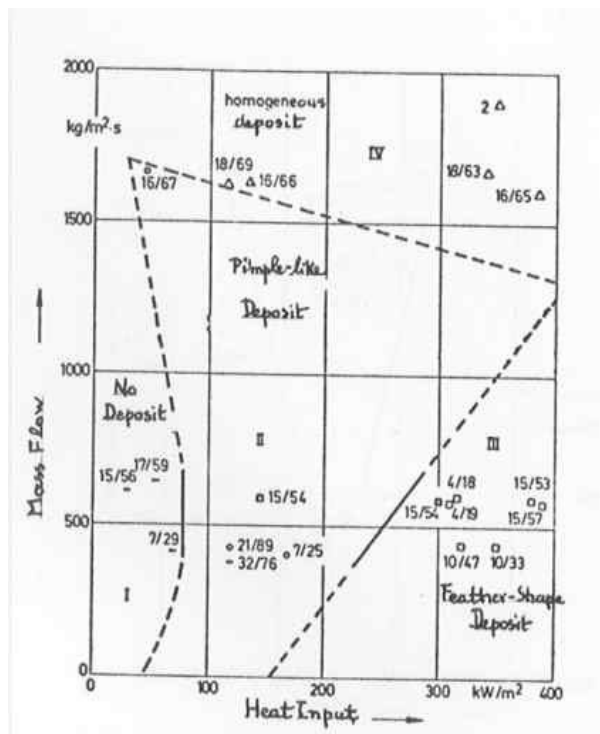


Figure 9.

Deposit phenomena in the test tubes with an inlet steam fraction of 0.58 up to 0.74; annular flow conditions

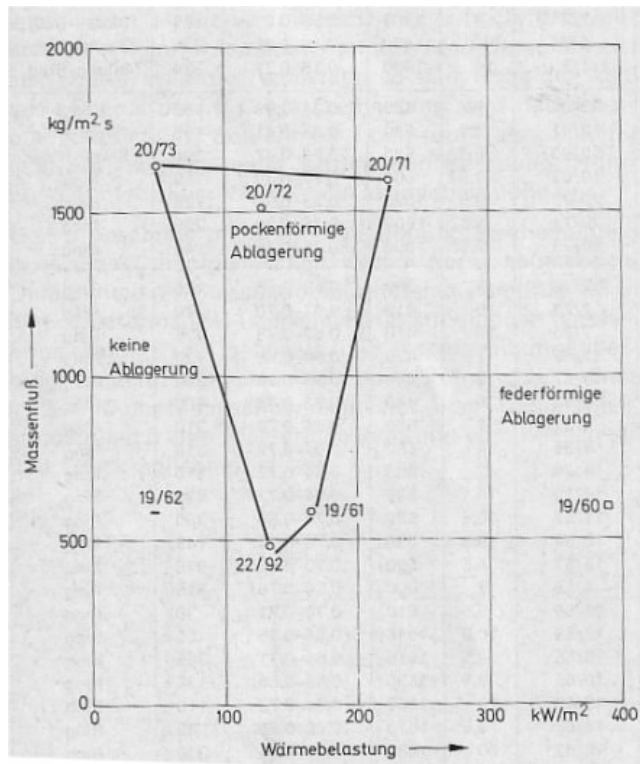


Figure 10.

Deposit phenomena in the test tubes with an inlet steam fraction of 0.34 up to 0.38; Plug and annular flow conditions.

3.3 Mechanism of deposit formation

In general, one may say that salt deposits form at locations where water is transforming to steam. The nucleate-boiling and "dry-out" processes have therefore a great influence upon the formation of deposits. In the nucleate-boiling process steam bubbles of various sizes are forming. If the tube surface is smooth, many small steam bubbles form randomly distributed over the surface. If the tube surface is not smooth (for example, due to defects in the material or high roughness), the bubbles form preferentially on the same nuclei. The amount of the bubbles and their size depends, of course, also partly on the heat-flux and the mass-transport. If the tube contain preferential locations for bubble formation, salts deposit at the edges of the steam bubbles by repeated evaporation of the water. Also undissolved particles will deposit there. In our opinion the pimple-type deposits form in this manner. Some of these pimples and a pimple cross-section are shown enlarged in Fig. 11.





Figure 11. Pimple shape deposits, formed under plug-flow and bubble-boiling conditions.

On the original steel surface a thin magnetite layer has developed which continues even above the hole-type attack. This indicates that at first a protective oxide layer has formed on the steel and that the steel was attacked under the pimple- type deposit during a later period. However, the attack is very small. We believe that by the mechanical action of the bubble-boiling process the dissolved corrosion products are carried from the hole and are deposited on the steel surface in form of needle-like and platelet-like iron oxides (Fig. 12).

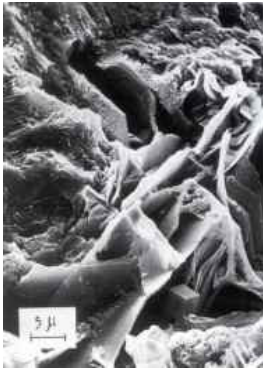


Figure 12. Platelet-shape and needle-shape corrosion products in the pimples. Scanning electron microscope pictures.

The pimple-type deposits are not yet found in tubes, in which "dry-out" occurs. Prior to the "dry-out" , heat transport occurs by nucleate-boiling at a great number of nuclei and finally by convection in the thin water-ring. The tube surface remains then also free from salt deposits.

With increasing mass-flow and increasing steam fraction, a homogeneous cover forms over the entire tube length, as can be seen in Fig. 9. This cover is not present behind large unevennesses in the tube surface, probably because of increased turbulence in the water film (Figs. 8 and 13).



Figure 13. Scanning electron microscope picture of the homogeneous deposit layer with a deposit-free path behind an obstacle.

It has been found that this cover and also the cover which forms under "dry-out" conditions consist of a mixture of BaSO_4 , CaSO_4 , $\text{BaCa}(\text{CO}_3)_2$, CaMoO_4 , KNaCO_3 , SiO_2 and a complex magnesium-aluminum-silicate-hydroxide, all stemming from traces of contaminations in the boiler water. Under the chosen experimental conditions and with a water-treatment with NH_3 no detrimental influence of these materials upon the oxide formation could be detected.

3.4 Conclusions from phase 1 of the investigations

1. Under the experimental conditions of this phase (clean tube surface, normal water composition, alkalisation with NH_3) no corrosion has occurred under any of the chosen, in the practice used thermohydraulic conditions, also not at the location of "dry-out". However, various types of deposits have been observed, i.e., pimple forms, feather forms and homogeneous deposits.
2. Pimple formation occurs under plug- and ring-flow conditions at a relatively low heat-input (100 to 200 kW/m^2), at which heat-transfer takes place by nucleate-boiling at selective nuclei locations. Only under the pimples is the steel attacked, but only to a minor degree.
3. Feather-like deposits originate at "dry-out" locations.
4. A homogeneous cover forms under annular flow conditions at the highest mass-flows within the entire range of the investigated heat-fluxes.

4. Phase 2 of the evaporator corrosion investigation

The experiments of phase 1 have shown that no serious corrosion phenomena occur under bubble-boiling conditions with normal water quality. It was intended for phase 2 to initiate distinct corrosion (so-called "on-load" corrosion) under bubble-boiling conditions. An evaporator corrosion investigation by Combustion Engineering (4 to 7) had already shown that corrosion is appreciably increased by dosing cooling-water salts if oxide suspensions are simultaneously dosed.

Since in drum-type boilers heat transfer occurs normally by bubble-boiling under bubble-flow conditions and probably also annular flow conditions, special attention was paid under these conditions to the initiation of "on-load corrosion". Heat-flux was therefore adjusted below the critical value. Since at circulation troubles (for example, by "carry-under") in a drum -type boiler the steam fraction in the evaporator can increase very appreciably and thereby also the danger of exceeding the critical steam fraction increases, some experiments were made with increasing steam fractions under "dry-out" conditions. The results of this phase are summarised in Table 2.

The test tubes Nos. 57/144, 65/137, 66/178, 56/88, 58/171 and 59/172 were tested in test section I and the other tubes of phase 2 in test section II with the double radiation furnace. The heat-flux listed in Table 2 applies to the upper radiation furnace. The heat-flux in the lower radiation furnace was set 25% lower.

For the initiation of evaporator corrosion seawater-salt concentrations of 0 to 27 mg/kg in the boiler water were chosen. In a circulation boiler the boiler water is in case of a large condenser leakage continuously blown down so that the salt concentration remains limited. The degree to which the blow down is made, depends on the size of the condenser leakage, the salt concentration in the cooling-water, the amount of condensate and the boiler content. The increase in salt concentration in the evaporator of a 150-MW boiler (evaporator content 100 t, condensate output 360 t/h, 2% blow down) was calculated for a condenser leakage of 30 l/h seawater. Fig. 14 shows that this salt concentration in the experimental boiler installation can occur in a circulation boiler already after 3 operating hours. A total condenser leakage of 30 l/h is not large, but difficult to find if it consists of several small leaks.

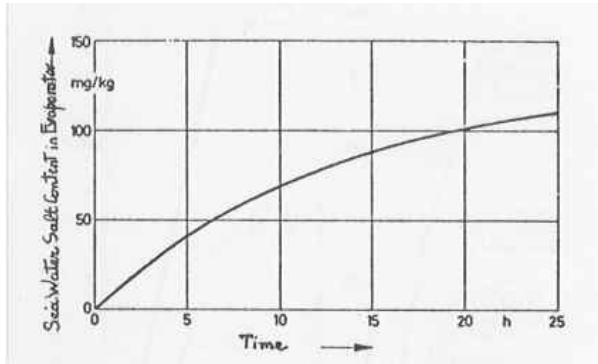


Figure 14. Salt concentration in an evaporator (150 MW). At a seawater leakage of 30 L/hr with a continuous blow off rate of 2%, condensate output of 360 t/hr. Evaporator content 100 t. The salt concentration increases up to an asymptotic value of 142 mg/kg.

4.1 Initiation of "On-Load" corrosion under conditions normally occurring in a circulation boiler

The dosings which were chosen for the experiments under water-ring-flow conditions, deviated to a small extent from those of the experiments under bubble-flow conditions. In both cases the highest salt concentrations given in Table 2, together with the oxide suspension, were adjusted during daytime for about 7 hours. Only under annular flow conditions a lower seawater salt concentration was maintained during the remaining 17h in order to maintain the once-formed salt layer.

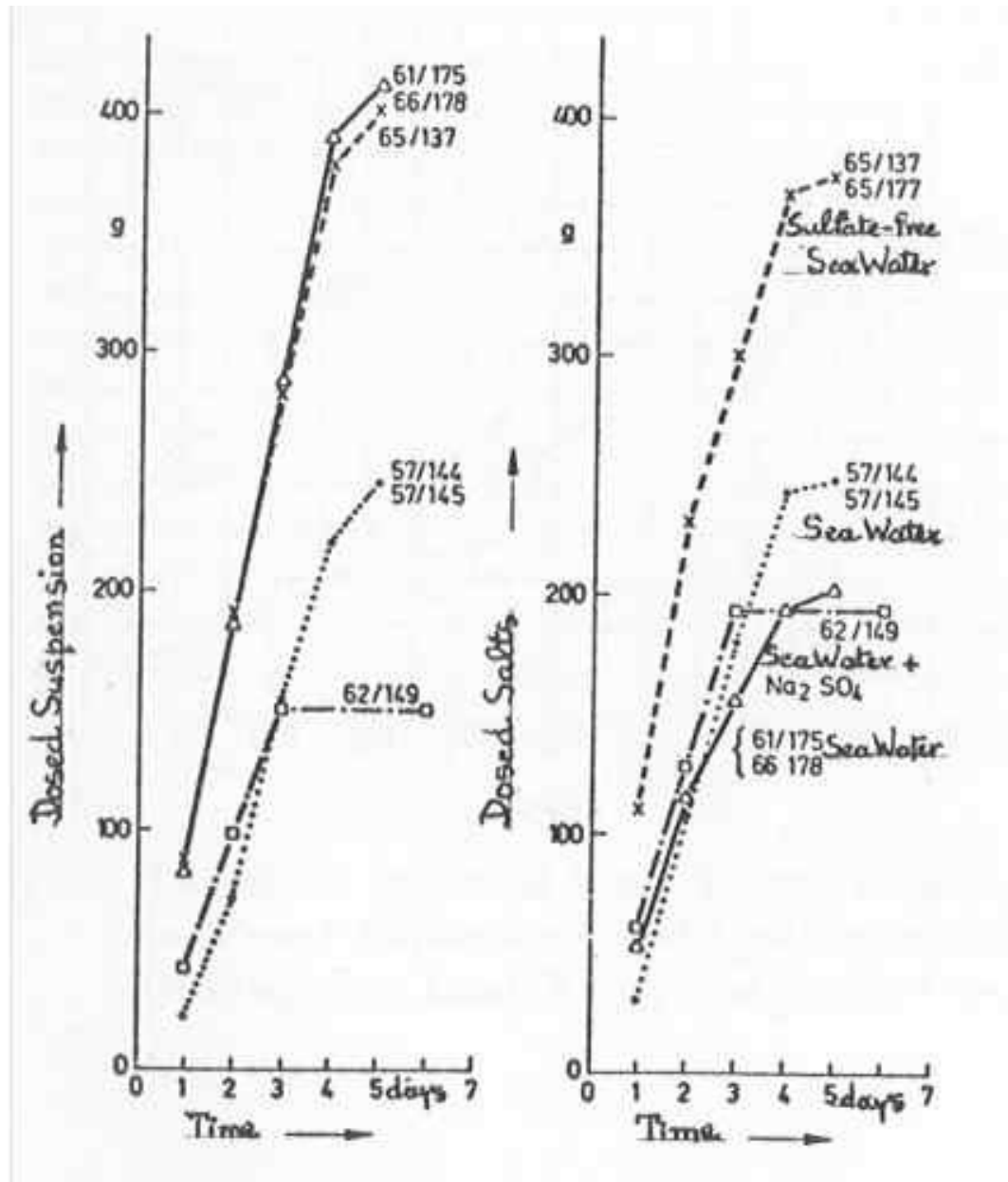


Figure 15. Total dosed amounts of suspension and salt during the experiments under annular flow conditions.

In Fig. 15 are shown the daily cumulatively dosed amounts of suspension and salts during the test periods of the annular flow experiments. The composition of the dosed synthetic seawater is listed in Table 3. The pH-value of the water in the separator decreased at high seawater dosings down to about pH = 5. During night the pH-value remained constant at the normal NH₃ adjusted value of 8.5 to 8.8. Table 2 gives the middle pH-values during salt dosing and the internal tube wall temperature reached at the end of the experiment. Table 4 presents a summary of the experimental results.

Table 4. Survey of results of tests with dosing of oxide suspension and sea water salts.

-: no; + weak; ++ distinctly present; +++ very distinctly present

Boiling conditions	Test tube no.	Corrosion	Hydrogen embrittlement	Salts	Oxide blistering and laminations	S-print	Cl-print
Annular flow with bubble boiling	57/144	+	-	+++	-	-	-
	57/145	+	-	+++	-	-	-
	61/175	+++	+++	+++	+++	+	++
	62/149	++	+	+	+	+++	-
	65/137	+	-	-	+	-	-
	66/178	+++	+++	+	+++	++	++
Bubble flow with bubble boiling	56/188	-	-	+	-	-	-
	56/142	-	-	+	-	-	-
	73/180	+++	+++	+++	+++	++	+
	77/184	+++	+++	+++	+++	++	++
	75/182	-	-	+++	-	-	-
	76/186	-	-	+++	-	-	-
Annular flow with "dry-out "	58/171	-	-	+	-	-	-
	58/174	++	-	++	+++	+	+
	59/172	-	-	-	-	-	-
	59/173	++	-	+	+++	-	-

It was found that the corrosion phenomena in the tubes which were tested under nucleate-boiling conditions did not display essential differences. At annular flow the tubes were strongly corroded (Table 2) already after 5 days and at bubble-flow only after 13 days. The criterion for terminating the tests was the attainment of a critically high tube temperature, in order to avoid tube rupturing. By measuring the tube wall temperature and the hydrogen content the corrosion process in the test tube could be followed. During the night when no dosings were made, the temperature decreased slightly due to rinsing away of deposits. However, as soon as the temperature remained constant or even increased during the night, this indicated accelerated corrosion, the result of which was that the test could be continued only for 2 or 3 days. Fig. 16 shows the trend of the temperature, H₂-production and pH -value during experiment No. 73. As the H₂-production indicates, corrosion does not stop instantaneously when seawater dosing is terminated.

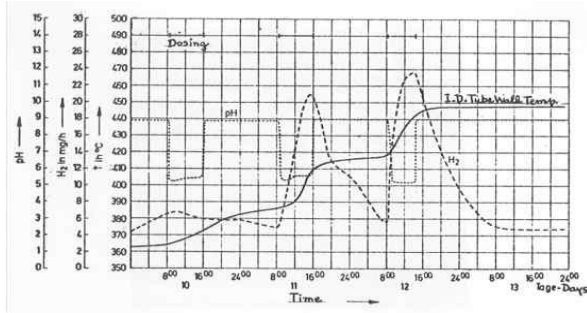


Figure 16. Trend of internal wall temperature, pH-value in water separator and hydrogen production during the last 3 days of experiment 73.

4.2 Examination of the corroded tubes

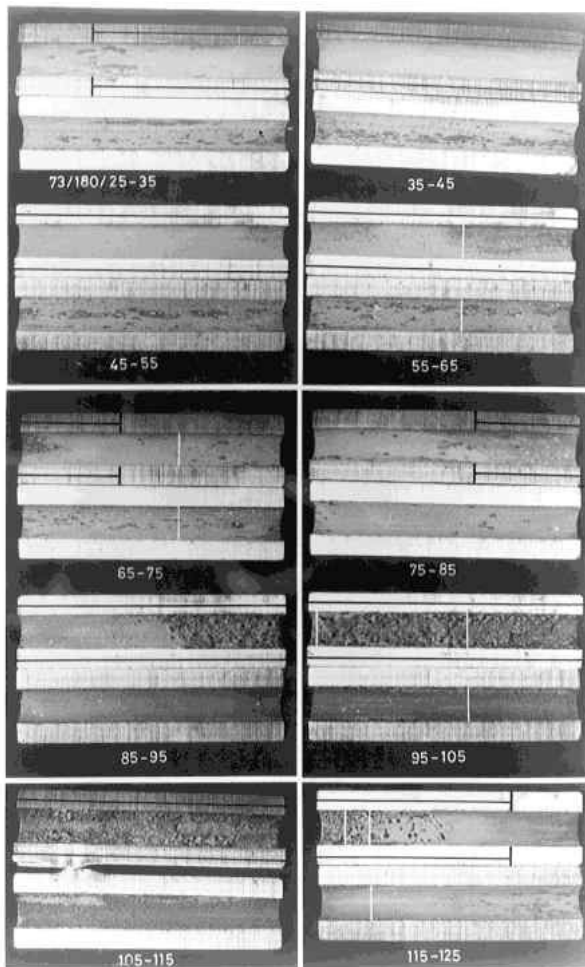


Figure 18. Split test tube 73/180. Thermohydraulic conditions: Steam fraction: 0.09; Mass flow: 1100 kg/m².s; Heat flux: 360 kW /m². Dosings into the boiler water: suspension 65 mg/kg; sea water 23 mg/kg. The white lines indicate the locations where samples were removed for microscopic examination. The black lines indicate the irradiated part.

Tube 73/180 had been tested under bubble-flow conditions. The heated side is most strongly corroded. It should be noted that pimple-like deposits have formed in the not directly heated side of

tube 73/180 at the height of the lower furnace, whereas the directly heated side was free of them. This is in agreement with the results from phase 1 where it had been found that pimples occur especially at lower heat-fluxes. At higher heat-fluxes the number of boiling-nuclei increases and therefore lowers the possibility for local pimple formation. For microscopic examination cross-sections were made at various locations of the tubes (indicated by white lines in Figs. 18). These revealed various phenomena.

Under the set-up conditions it is not necessary to adjust the heat-flux in order to obtain porous deposit layers. Also outside the sections, which were heated by the furnaces, a porous, but somewhat thinner layer was found. In the section with heat-input so-called steam "chimneys" are present in the porous layer, which is the result of the heat transfer process in the layer. The porous layer is filled with water. At certain locations of nuclei bubble-boiling (column-boiling) occurs whereby steam chimneys are formed by the escaping steam (Fig. 19).

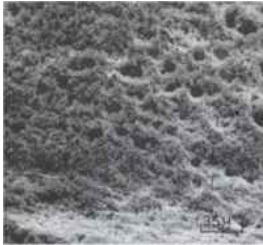


Figure 19. Scanning electron microscope pictures of the porous oxide deposit layer. The steam chimneys are distinctly recognisable.

When in addition to oxide also salts were dosed, it was found that a network of boiler water salts forms on the irradiated tube surface. On the non-heated parts the porous oxide deposit formed, but salts were not present (Fig. 20).

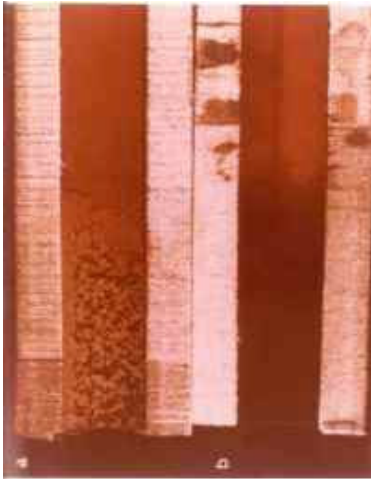


Figure 20. Longitudinal sections of tube 46/88: a) the heat input part; b) the non-heat-input part. The loose porous top layer has been rinsed off with tap water so that the network of salts on the heat-input section became visible.

The formation of such a network of salts can be explained, as follows. (Fig 21).

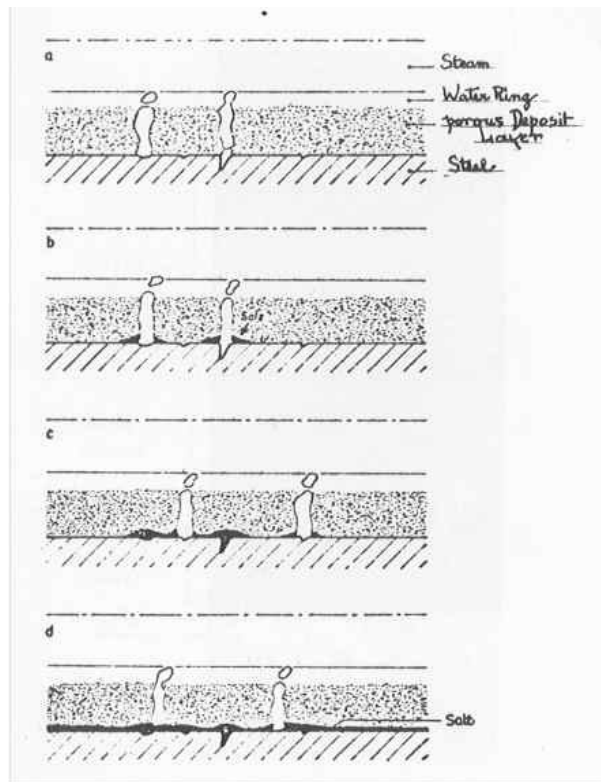


Figure 21

Model for the formation of salt deposits in a porous layer of iron oxides. The salts are conducted to the bottom of the steam tunnel, where they precipitate when their solubility is exceeded.

The water which evaporates at the location of the bubble nuclei, is carried there by the porous layer of the oxide deposition. At the edge of the steam chimney salt solution will evaporate on the tube wall until super saturation takes place. Under these circumstances less soluble salts, such as sulphates, silicates and phosphates will deposit. At this location the heat passage will diminish so that the chimney forms at another, more favourable, location. In this manner a salt layer is gradually forming on the tube wall. In addition, the temperature of the tube surface will thereby increase.

Thus it was found in experiment 57 that a compact salt layer has formed without the occurrence of significant corrosion (Fig. 22).

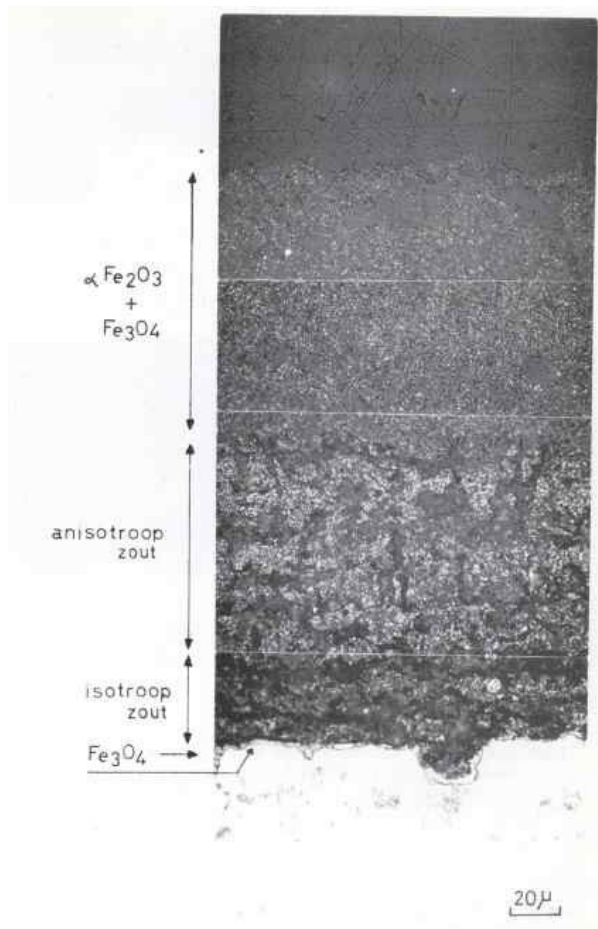


Figure 22.

Longitudinal section through tube 57/ 145/ 99. On the top of the 1 to 2 micron thick magnetite layer are a dark isotropic salt layer (40 microns thick), an anisotropic salt layer (80 microns thick) and a porous layer of hematite and magnetite



Figure 23.

Detailed pictures of the dark salt layer on top of the thin magnetite layer in tube 57/145/98-100. The pearlite structure of the steel can be recognised in the dark-grey salt layer, which points to attack of the magnetite by the salt layer.

Over the entire tube length, on the heated and to a lesser extent on the non-heated side, a two-part salt layer is present under the porous, about 100 micron thick deposit. On the steel are, above each

other, an about 1 to 2 micron thick Fe_3O_4 layer, a dark isotropic salt-containing layer (40 micron), an anisotropic light-gray salt-containing layer (80 micron) and the porous deposit of Fe_3O_4 and $\alpha\text{-Fe}_2\text{O}_3$. It is noteworthy that the original pearlite microstructure of the steel can still be recognised in the dark-gray layer, immediately on top of the thin, gray magnetite layer (Fig. 23). The gray salt must have transformed the formed magnetite during the test period into another product in such a manner that the texture of the pearlite became again recognisable. In former experiments and also in the investigation of tubes from operation it had already been found that with exact polishing the pearlite structure is still visible in the magnetite. The deposit layers were examined in more detail by scanning electron microscopy and X-ray analysis (Fig. 24).

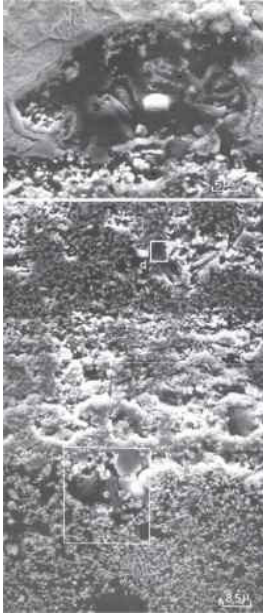


Figure 24. Scanning electron microscopic pictures of sample 57/ 145/ 96. In the dark salt layer the elements Mg, S and Fe were found. In the outer layer is, in addition, Ca found.

It was found that the salt immediately above the thin magnetite layer is rich in Mg, S and Fe whereas the salt layer which is more toward the outside contains, apart from Mg and S, distinctly more Ca and Fe. By X-ray diffraction the following salts have been found: CaSO_4 , $\text{Mg}(\text{OH})_2$, Na_2SO_4 , and MgSO_4 , $\text{Mg}(\text{OH})_2$, $2\text{MgCO}_3 \cdot 6\text{H}_2\text{O}$. Due to these salt deposits the tube wall temperature had gradually increased from 355 to 374 °C.

It was found in this series of experiments that the dosing of oxide suspension increased the pH-decrease. We assume that the oxides promote the hydrolysis of MgCl_2 to $\text{Mg}(\text{OH})_2$ which must be confirmed by a more detailed investigation. We have furthermore found that the tubes are strongly attacked if the oxide suspension which is dosed in addition to the seawater, is added in greater amounts. The pH decreases then also more strongly. Tubes 61/175 and 66/178 were so strongly corroded that even methane embrittlement had occurred. In Figs. 25 to 27 some microscopic pictures of the oxide layers have been made.

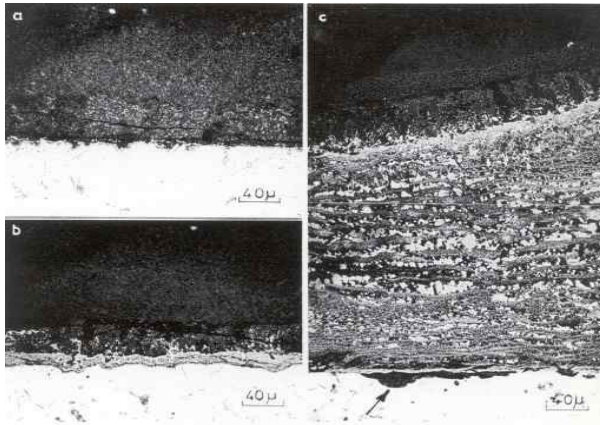


Figure 25.

Sections through a corroded tube with 4 stages of "on-load corrosion". · On top of the thin magnetite layer a porous oxide layer (stage 1) is formed in which salt has deposited (stage 2). · Attack of the thin magnetite layer and formation of the top layer (stage 3). · Thick crust of layered oxide under the top layer (stage 4)

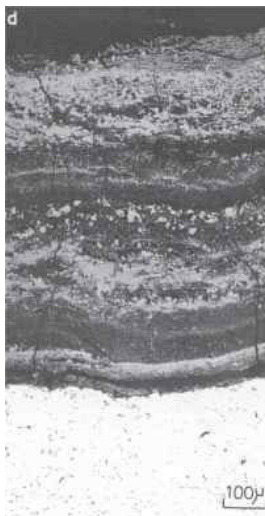


Figure 26.

Section through samples at locations 105/ 12. On the irradiated side (d) the oxide layer is very porous and there are coarse magnetite crystals. On the not directly heated side the oxide layer is finely laminated.

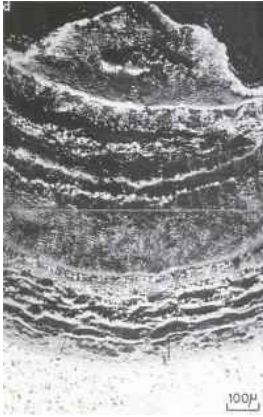


Figure 27.(right)

Section of tube 73/ 180 at locations 117/ 12 (d). At the middle of the side with the greatest heat-input very porous oxide has formed. At the location with less heat-input (end of the oven, d) the oxide is finely laminated.

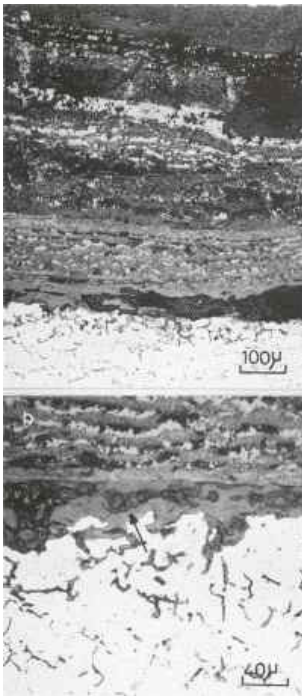


Figure 28.

Sections through samples from tube 61/ 175. Between the oxide and the steel corrosive salt has been deposited (a and b).

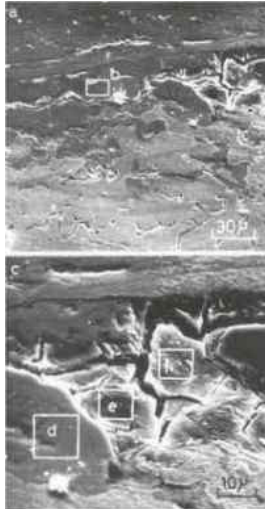


Figure 29.

Scanning electron microscope pictures of sample 61/ 175/ 103. It is found that the composition of the grey salt and of the clay-like structure is alike. Furthermore, the elements S and Cl are present.

If the pH-value does not fall too low, for example, to 5.3 in experiment 57, no severe corrosion is observed. Nevertheless, it is found that the occurrence or non-occurrence of corrosion does not directly depend on the pH-value in the boiler water. In experiment 65 in which dosing of sulphate-free seawater and oxide suspension was associated with a pH-value decrease down to 5.0, no distinct corrosion has occurred. Tube wall temperature remained low, which, in our opinion, was caused by the fact that the dosing salts contained no sulphate. In experiment 62 to which Na_2SO_4 was added to the dosed seawater, the tube wall temperature rose to the high value of 476 °C and the tube was distinctly corroded.

In the study of the corroded sample test tubes four stages of the so-called "on-load corrosion" are noted, of which especially Fig. 25 gives a good survey:

As first stage the formation of a porous layer of iron oxide particles may be named.

In this "sponge" of loose oxide particles salt (especially sulphates) will precipitate at the locations of nuclei due to the nucleate-boiling process. The boiling nuclei are shifting as a result of local salt deposits so that gradually a uniform salt layer is formed over the tube surface (Fig. 25a).

Under this salt layer the thin, in Fig. 25a still present) magnetite layer is attacked and a thicker porous layer is formed (Fig. 25b). This porous layer is always observed on the layered oxide crusts described in stage 4 and will subsequently be designated as top layer.

After formation of the about 20 micron thick, porous top layer, accelerated corrosion begins (Fig. 25c). In this stage various phenomena are noted which are important for explaining the corrosion mechanism:

1. The oxide crusts are strongly laminated. Such a lamination can be explained by the scaling of the oxide from the metal surface. On the tube halves which had not been directly heated a fine layered oxide crust has formed; at the same height in the tube, but on the heated half the oxide is more porous and there are sometimes very coarse magnetite crystals present (Figs. 26 and 27).
2. At the oxide/metal interface pitting is sometimes observed. The holes are filled with iron rust. Such an attack is indicated in Fig. 25c by an arrow. In the most heavily corroded tubes a stronger bluish-gray bond mixed with iron oxides is frequently found between the coarse-laminated oxide crusts and the steel (Fig. 28). This material is frequently anisotropic and with the aid of energy-dispersive X-ray analysis S and Cl were especially indicated in addition

to iron (Fig. 29). It differs distinctly from the salt deposit on the top layer (Fig. 24) since the element Mg is not present.

- It is found that strongly corroded tubes give distinctly positive sulphide- and chloride-prints, which is also in agreement with the above described X-ray analyses. Chloride and sulphide were directly present only on the steel surface and were recognisable in the Baumann prints as sharp lines.

It is to us not yet entirely clear how the mechanism of the accelerated corrosion should be interpreted in order to be able to explain all the above named phenomena. Because the internal temperature in this stage has already raised to high values (450 °C), it is not probable that the oxide crust under the top layer could still contain water or even concentrated salt solution. Only at the beginning of the accelerated corrosion when the tube wall temperature is still rather low, concentrated electrolyte could form, for example, HCl or FeCl₂. The low-solubility salts then deposit on the outside of the top layer. In the case of seawater leakages HCl, formed by hydrolysis of MgCl₂, could concentrate under this salt- and top-layer and attack the magnetite which formed immediately on the steel. The Fe(II)-chloride which is formed thereby, will remain present in the oxide crust and allow corrosion to continue. A hint for the correctness of this mechanism is furnished by extended autoclave experiments with Fe(II)-chloride solutions which showed that steel is strongly attacked in this environment with formation of laminated layers. Due to the high pressure stresses which formed in the layer during its growth and the bad adhesion of the oxide to the steel the oxide regularly flakes from the steel. If the oxide breaks off just before the tube is taken operation, the chloride in the crust will allow the bare steel surface to rust. The steel will then be attacked by pitting, and loose, porous corrosion products will form.

With progressing corrosion only steam (with or without Cl) or, perhaps, even salt-melt, can exist in the laminated oxide because of the high temperature. In case of heavy corrosion a sulphide -rich and chloride -rich phase will be found directly on the steel surface, and the presence of sulphide may indicate that at the observed "on-load corrosion" a sulphate-reducing reaction does also occur. A sulphate-reducing reaction mechanism is known in corrosion by salt-melts, as in fireside attack. It does not appear impossible that at "on-load corrosion" the reactions can proceed in a similar manner due to high concentration of salts in the oxide crusts. Further laboratory experiments are then also necessary in order to determine if laminated oxide layers are formed also in salt-melt or in steam with HCl at high pressure.

4.3 Influence of increased steam fraction

Table 2 contains a summary of the conditions for determining the influence of an increase in the steam fraction and of the "dry-out" (Experiments 75, 76, 58 and 59). Although the same dosings were chosen as in the preceding experiments, the pH-value in the outcoming water decreased less.

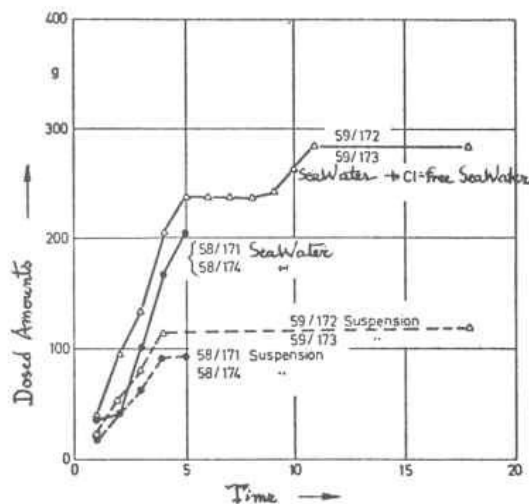


Figure 30.

Total dosed amounts of suspension (-----) and salt (_____) during the experiments under "dry-out" conditions.

Fig. 30 is again cumulatively showing the dosings for the test periods during the "dry-out" experiments since in experiments 58 and 59 small amounts of salts were dosed also during the night.

Table 4 presents the results of this series of corrosion experiments. In the experiments under "dry-out" conditions corrosion did occur, but no distinct hydrogen embrittlement, that is, not as much as in the tests under nucleate boiling conditions, in which also larger amounts of oxides were dosed and the pH dropped to lower values.

Probably because of the low pH-value decrease -which is possibly connected with the adjusted higher steam fraction of 0.2 -no distinct corrosion has occurred in the experiments 75 and 76. Although a salt-deposit layer formed, the above described stage of attack of the thin magnetite layer and the formation of the top layer were not obtained. We consider it likewise possible that the salt layer which forms at this higher steam proportion has a more separating effect which renders the concentration of dissolved salts under the solid salt crust difficult.

4.4 Conclusions from phase 2 of the investigations

- The test tubes could be quickly contaminated, by dosing of oxide suspensions under annular flow conditions. Heat-flux promotes the deposition of oxides on the tube surface, but is not necessary for it. If salt is dosed in addition, it deposits in the loose porous layer on the tube surface by means of the so-called column-boiling process.
- It is found that in evaporator corrosion under the thermo hydraulic conditions which normally occur in circulation boilers four stages can be distinguished:
 1. Formation of a porous deposit layer.
 2. Precipitation of salts in the porous layer. The salts are deposited directly on the tube surface.
 3. Attack on the initially protective, about 2 micron thick oxide layer and formation of a so-called top layer.
 4. Occurrence of increased corrosion under the top layer; a layered oxide is formed, which fineness decreases with increasing salt concentration
- In order to initiate the formation of layered oxide crusts, a salt layer must have formed on the tube surface and the pH-value of the boiler water must be sufficiently low, depending on the boiler conditions and the water composition.
- In the fourth stage a more porous oxide with coarse magnetite crystals is formed in the crusts at high concentrations of the dissolved salt. Sometimes a sulphide- and chloride-rich phase is then observed at the oxide/metal interface. It appears that under otherwise the same experimental conditions corrosion is weaker at a steam proportion of 0.2 than at a steam proportion of 0.1.
- In the cases in which heavy "on-load corrosion" was observed, the latter was associated with hydrogen embrittlement.

5. References

1. J.G. Collier Nuclear Power (6), 61-66, (1961)
2. J.G. Collier Nuclear Power (7), 64-67, (1961)
3. Rosler, USAEC Rapport WAPD-TM-658 (1967)
4. H.A. Klein, J.K. Rice, 1966. Research study on internal corrosion of high pressure boilers. Transactions of the ASME, Journal of Engineering of power, juli 1966, 232-42.
5. P. Goldstein, J.B. Dick, J.K. Rice, 1968. Internal corrosion of high pressure boilers. Transactions of ASME, Journal of Engineering of power, paper no. 66-WA/BFS-1.
6. P. Goldstein, 1968. A research study on internal corrosion of high pressure boilers. Journal of Engineering for Power, januari 1968, 21-37
7. P. Goldstein, C.L. Burton, 1969. A research study on internal corrosion of high pressure boilers, final report. Journal of Engineering for Power, april 1969, 74-101